Supercontinuum Generation with Femtosecond Self-Healing Airy Pulses

Craig Ament, Pavel Polynkin,* and Jerome V. Moloney

College of Optical Sciences, The University of Arizona, Tucson, Arizona 85721, USA
(Received 5 July 2011; published 5 December 2011)

We report experiments and numerical simulations on supercontinuum generation with femtosecond Airy pulses in a highly nonlinear optical fiber. The ability of the Airy waveform to regenerate its dominant intensity peak results in the generation of distinct spectral features. Airy pulses and other self-healing temporal waveforms may be useful for the generation of spectra with desired properties.

The dramatic spectral broadening experienced by intense optical pulses in nonlinear media, commonly known as supercontinuum generation, is a result of the complex interplay between linear dispersion and instantaneous and delayed nonlinearity in the medium [1]. Microstructured optical fibers are particularly well suited for supercontinuum generation because the nonlinearity and dispersion landscape in microstructured fibers can be altered by the design of the waveguide structure [2].

Although supercontinuum generation in optical fibers has been extensively studied in the past [3], the overwhelming majority of prior studies utilized intense optical pulses with symmetric and compact temporal profiles such as Gaussian or hyperbolic secant pulses. There have been several reports on the optimization of supercontinuum generation via pulse shaping [4–6]. However, this approach remains insufficiently explored.

Recently, a new kind of optical pulse has been introduced to optics. These so-called Airy pulses have their field envelopes described in terms of Airy functions of time. These pulses are temporal analogues of Airy beams [7]. Like Airy beams resist diffraction and self-bend, Airy pulses resist dispersion and their dominant intensity peaks accelerate on propagation. In addition, Airy pulses are able to regenerate their dominant intensity features should those features be selectively attenuated or distorted. All of the above features are linear effects.

An ideal Airy pulse would maintain the width and the amplitude of its dominant peak indefinitely. It can be shown that Airy pulses are the only waveforms that have this property in a linear dispersive medium. However, the ideal Airy waveform is not square integrable; thus, it cannot be realized experimentally. What can be practically realized is the apodized Airy pulse, which is described in terms of the product of an Airy function and an apodization envelope. Apodized Airy wave packets retain the dispersion resistance property of their ideal counterparts, but only for a finite propagation distance, over which the amplitude of the dominant peak is gradually decreasing on propagation. The dispersion resistance and self-regeneration of the exponentially apodized temporal Airy wave packet are illustrated in Fig. 1. Airy pulses have been

experimentally realized and their properties have been studied in linear [8] and nonlinear [9] regimes.

The ability of Airy pulses to self-heal makes them potentially useful in the context of supercontinuum generation. With a symmetric and compact input pulse in the anomalous dispersion regime, which is commonly used for the generation of broadest continua, the spectral evolution of the pulse largely ends when the pulse is transformed into one or several fundamental solitons. The excess energy in this case is shed into dispersive waves [10]. In the case of the self-healing Airy pulse, the generation of new spectral components may continue after the dominant peak of the waveform has produced solitons and dispersive waves and removed itself from the continuum-generation process.
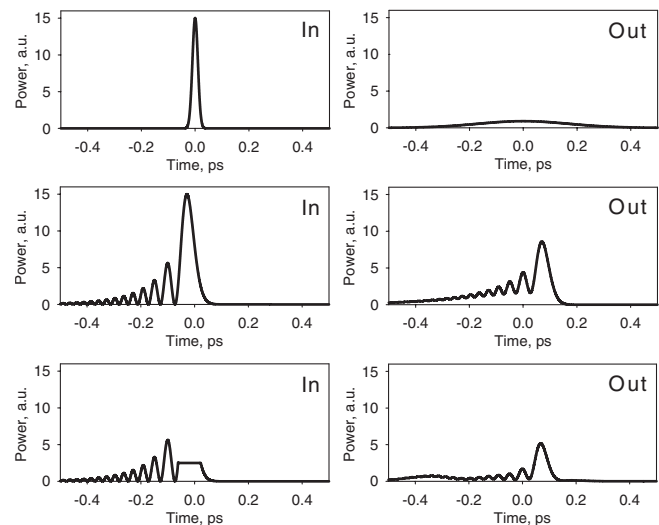

FIG. 1. Top row: Simulation of a Gaussian pulse propagating in a linear medium that has a second-order dispersion only shows a severe pulse spreading on propagation. Middle row: The input pulse is an exponentially apodized Airy pulse with the same optical bandwidth as that of the Gaussian pulse above. Propagation through the same medium leaves the dominant peak of the waveform largely intact. Bottom row: The dominant intensity peak of the input Airy pulse is cutoff at a level of one-sixth of the peak value. The feature is restored on propagation through the same dispersive medium as above.

Under the right conditions, the dominant feature of the Airy waveform will be regenerated. At that point, it will propagate with a velocity different from that of the dominant peak of the original pulse, affecting the placement of the newly generated spectral components. Thus the use of Airy pulses and other sophisticated self-healing temporal waveforms may allow for control over the generated supercontinuum by linear optic means.

In this Letter, we report the results of a numerical and experimental study of supercontinuum generation with Airy pulses in a microstructured optical fiber. Our results show that the self-healing property of the pulse, under certain conditions, results in nontrivial cyclic behavior. The dominant feature of the pulse creates a solitondispersive-wave pair, regenerates itself, then creates another soliton-dispersive-wave pair, and so on. Such propagation dynamics results in the generation of distinct features in the output optical spectrum.

An Airy pulse is created by imposing a cubic phase onto the spectrum of an input Gaussian pulse. The cubic phase can be positive or negative, which corresponds to the Airy pulse with the tail lagging behind the dominant peak of the pulse or vice versa. The orientation of the tail of the pulse with respect its peak has two important consequences. First, linear third-order dispersion, which has a particular sign, will add to or subtract from the cubic phase of the input Airy pulse, resulting in the extension or reduction of the dispersion-resistant propagation range of the pulse. In fact, the generation of Airy waveforms from input Gaussian pulses, as a result of propagation through a fiber with third-order dispersion, has been described as early as 1979 [11], much before the concept of the dispersion-resistant Airy pulse had been proposed. Second, solitons produced through the collapse of the dominant peak of the Airy pulse generally tend to lag behind the main pulse waveform. Thus for the case when the tail propagates ahead of the main peak of the pulse, the generated solitons cleanly detach themselves from the waveform and leave the self-healing of the pulse unaffected. When the tail of the pulse propagates behind its main peak, the generated solitons pass through the tail and interfere with the self-healing.

The parameters of the optical fiber used in the simulations throughout this report match those of the fiber used in our experiments. The nonlinear coefficient γ of the fiber equals 0.11 $(W \cdot m)^{-1}$. Its dispersion profile, as specified by the fiber manufacturer, is shown in Fig. 2. In the simulations, the fiber dispersion is fitted by a 10-order polynomial in optical frequency.

The input Airy pulses are numerically generated by imposing a cubic spectral phase of minus or plus 60 000 fs^3, onto the spectrum of a 24 fs long, transform-limited Gaussian pulse with the spectrum centered at 800 nm wavelength. Under these conditions, the dominant peak of the pulse contains about one half of the total energy
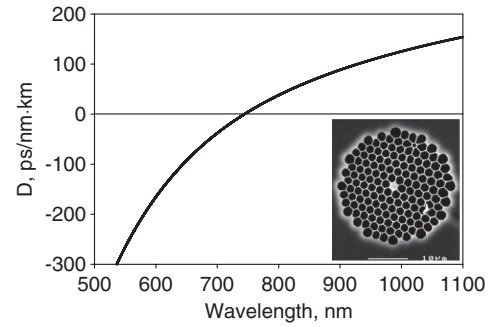

FIG. 2. Fiber dispersion as a function of wavelength. The inset shows a scanning electron micrograph of the guiding region of the fiber provided by the fiber manufacturer.

of the waveform. The pulse evolution is simulated by using the numerical model adapted from [12]. In the model, the optical field is assumed to remain linearly polarized throughout the entire propagation in the fiber.

Figure 3 shows the temporal and spectral outputs from a 1 m long nonlinear fiber with the parameters listed above, for the case of an input Airy pulse with peak power of 1.5 kW and a negative cubic spectral phase equal to $-60\,000$ fs^3. The tail of the waveform in this case propagates in front of its main peak. Three soliton-formation events are evident from the side-by-side examination of the temporal and spectral shapes of the pulse as it propagates through the fiber. All three solitons are produced through the reshaping of the main intensity peak of the Airy pulse, which recreates itself after each soliton-formation event. After their formation, solitons and dispersive waves remain essentially invariant on propagation, except for the continuous frequency redshifting of the soliton spectral peaks caused by higher-order dispersion and Raman effect. The number of the peak-regeneration cycles is limited by the degree of apodization of the input Airy waveform.

The redshifted solitons gradually slow down and may catch up with dispersive waves in time domain. In that
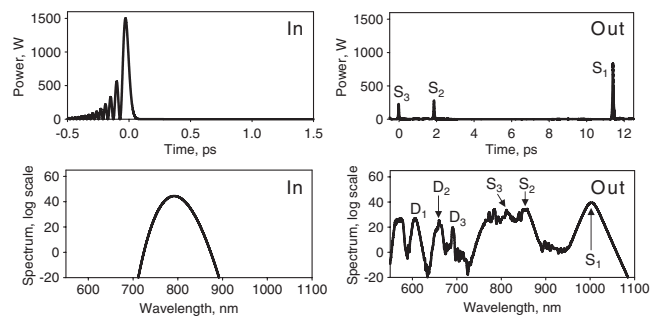

FIG. 3. Top row: Input and output temporal waveforms for an Airy pulse with $-60\,000$ fs^3 cubic spectral phase propagating in a 1 m long nonlinear fiber with the parameters described in the text. Bottom row: Corresponding spectra. Solitons and dispersive waves are marked with letters S_i and D_i, where the subscript indicates their order of appearance.

case, the cross-phase modulation induced by the intense soliton field causes the redistribution of the energy of the dispersive wave and results in the appearance of an additional blueshifted spectral peak, as described in [13]. The left-most peak at 570 nm in the bottom right panel of Fig. 3 is the result of such an interaction between the first emitted soliton S_1 and the dispersive wave D_1.

The placement of the spectral peak corresponding to a particular dispersive wave is determined by the wavenumber matching between the dispersive wave and the higher-order soliton that undergoes fission, in the immediate vicinity of the point where the peak power of the soliton in the highest [14]. For the case of a fundamental soliton, the matching condition has the following form:

$$\sum_{n\geq 2}\frac{\beta_n(\omega_S)}{n!}(\omega_D - \omega_S)^n = \frac{\gamma P_S}{2}, \qquad (1)$$

where $\beta_n(\omega_S)$ are the higher-order dispersion coefficients of the fiber at ω_S, the optical frequency of the soliton, ω_D is the center frequency of the dispersive wave, γ is the nonlinear parameter of the fiber, and P_S is the soliton peak power. Although (1) is only valid for fundamental solitons, it is frequently used for estimations of the dispersive wave placement in the cases of solitons of higher order. The center wavelengths of the three generated dispersive waves in the case shown in Fig. 2 are, in order of their appearance, 600, 668, and 690 nm. The estimates based on the formula (1) are 580, 639, and 663 nm. These estimates are consistently lower than the values derived from the simulations. The poor agreement may be caused by, among other things, the accelerating nature of the Airy waveform, for which case the condition (1) is overly simplified.

Figure 4 provides a closer look at the first two soliton-formation events. The top left panel shows the pulse after it propagated 6 cm through the fiber. At that point, the main peak of the input pulse has transformed itself into a
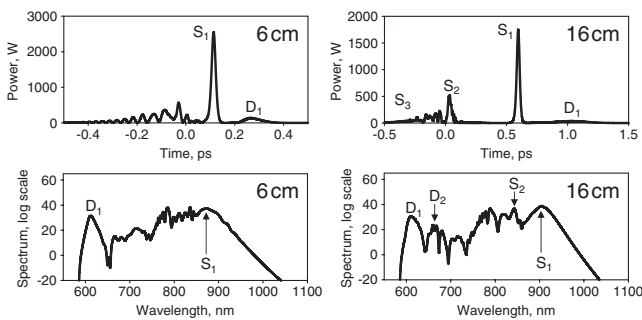
higher-order soliton that subsequently underwent fission and shed a dispersive wave. The main peak of the waveform is nearly regenerated and ready to produce another soliton. The top right panel shows the pulse profile after 16 cm of propagation. The regenerated main Airy peak has just created another soliton.

In the spectral domain, the soliton and dispersive wave created through the first collapse of the main Airy peak are straightforwardly identifiable at both 6 cm and 16 cm. Spectral features resulting from the second soliton-formation event are not as obvious. To properly identify them, we computed a Fourier transform of the portion of the temporal waveform at 16 cm that contained the peak marked by S_2.

In the above example, the Airy pulse had a negative value of the cubic spectral phase, in which case the tail of the Airy waveform propagated in front of its main peak. The solitons and dispersive waves generated from the main peak of the pulse lagged behind the waveform and did not interfere with its ability to self-regenerate.

The case corresponding to the opposite sign of the cubic spectral phase is shown in Fig. 5. As in the previous case, the dominant intensity peak of the input Airy pulse relatively quickly reshapes itself into a higher-order soliton which subsequently morphs into a fundamental soliton and emits a dispersive wave. However, in this case, the generated soliton passes through the tail of the Airy pulse and perturbs the phase of this waveform via cross-phase modulation. As a result of that perturbation, the Airy waveform loses its ability to regenerate its main peak. Two additional solitons are still produced by the remaining part of the pulse, but these features originate from the secondary peaks of the waveform, and not from the rebuilt dominant intensity feature. Only one distinct dispersive-wave peak is evident in the output spectrum in this case. As in the case with negative cubic phase, the leftmost feature in the output spectrum results from the interaction of the first emitted soliton with its own dispersive wave.

In order to validate the pulse propagation scenario put forth above by numerical simulations, we conducted
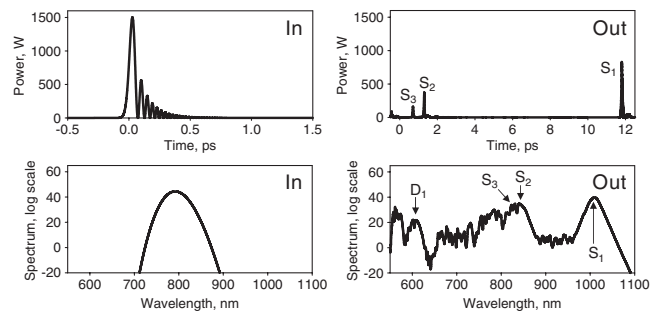

FIG. 4. Top row, left: Airy pulse with $-60\,000$ fs^3 cubic spectral phase after 6 cm propagation in the fiber. The main peak of the Airy waveform has produced a soliton-dispersive-wave pair and is nearly regenerated. Right: Same after 16 cm propagation. The regenerated main peak of the pulse has produced another soliton-dispersive-wave pair. Bottom row: Corresponding spectra.

FIG. 5. Input Airy pulse with $+60\,000$ fs^3 cubic spectral phase propagates in 1 m long nonlinear fiber. Top row: Temporal input and output waveforms. Bottom row: Corresponding spectra. Only one distinct dispersive-wave peak is produced.
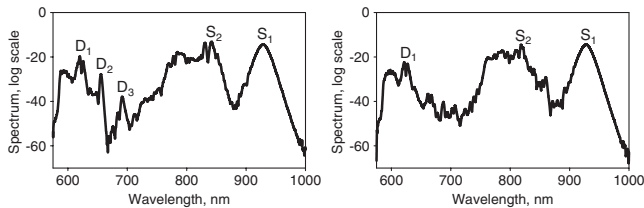
FIG. 6. Supercontinuum spectra recorded at the output of a 1 m long microstructured fiber with the parameters closely matching those used in the simulations. The case with the input Airy pulse with a negative cubic spectral phase equal $-60\,000$ fs^3 (left) results in the generation of three distinct dispersive-wave features. The case with the same but opposite spectral phase (right) results in the generation of only one distinct dispersive wave.

experiments on supercontinuum generation with Airy pulses in a nonlinear fiber. In the experiments, the input Gaussian pulses are generated by a modelocked Ti:sapphire laser oscillator operating at 800 nm center wavelength and 80 MHz pulse repetition frequency. Pulses out of the oscillator are dechirped to about 24 fs duration, which is close to the transform limit, using a dispersive prism pair. Airy pulses are produced by imposing a cubic spectral phase onto these transform-limited Gaussian pulses, using a computer-controlled pulse shaper (Silhouette$^{\mathrm{TM}}$ by Coherent). The maximum cubic phase attainable in our setup is limited to plus or minus $60\,000$ fs^3, which matches the magnitude of the cubic phase used in the simulations.

The shaped pulses are coupled into a 1 m long nonlinear fiber with the parameters that closely match those used in the computer simulations discussed above. The mode-field diameter of the fiber is about 1.4 μm, its estimated nonlinear coefficient γ equals 105 $(\mathrm{W} \cdot \mathrm{m})^{-1}$, and the zero dispersion wavelength of the fiber is 745 nm. The coupling efficiency of the shaped laser pulses into the fiber in our setup is about 20%, which corresponds to 0.25 nJ of maximum pulse energy coupled into the fiber. The input pulse energy is varied by adjusting the focusing of the fiber-coupling arrangement. The supercontinuum spectra at the output from the fiber are recorded using an optical spectrum analyzer.

Two examples of experimentally measured spectra are shown in Fig. 6. In both cases shown, the energy of input Airy pulses equals 0.12 nJ. The amount of the cubic spectral phase imposed by the pulse shaper in order to generate these waveforms is $-60\,000$ fs^3 (left) and $+60\,000$ fs^3 (right). Under these conditions, the estimated peak power of the Airy pulses coupled into the fiber is 1.5 kW, the same as that in the simulations.

For the case with a negative cubic spectral phase, the generated supercontinuum spectrum has three distinct and approximately equidistant dispersive-wave peaks, in qualitative agreement with the simulation shown in Fig. 3. For the case with a positive cubic phase, only one distinct

dispersive-wave feature is produced, again in agreement with the simulations. In both cases, the left-most peak in the spectrum is due to the interaction between the first emitted soliton and its own dispersive wave. The quantitative discrepancy between the experiment and the simulations is likely due to the incomplete knowledge of the fiber parameters as well as to the residual fiber birefringence not accounted for in the model.

In conclusion, we conducted experiments and numerical simulations on supercontinuum generation with self-healing Airy pulses in a nonlinear fiber. The pulse propagation dynamic is found to be different for the cases when the tail of the waveform propagates in front of and behind its main peak. In the first case, the dominant peak of the pulse recreates itself after several soliton-formation events, resulting in the generation of distinct dispersive-wave features in the output spectrum. In the second case, the soliton generated from the first collapse of the main peak passes through the tail of the waveform and disrupts its ability to self-regenerate. The results of the modeling are in qualitative agreement with the experiments. The dispersion resistance and self-healing property of temporal Airy waveforms offer new means of control over ultrafast nonlinear optic interactions. The introduction of these pulses may have similar impact on the ultrafast laser science as the impact that the invention of the diffraction-resistant Bessel beams [15] had on classical optics.

---

*ppolynkin@optics.arizona.edu

[1] *The Supercontinuum Laser Source: Fundamentals with Updated References*, edited by R. R. Alfano (Springer, New York, 2006).

[2] T. A. Birks, D. Mogilevtsev, J. C. Knight, and P. St. J. Russell, IEEE Photonics Technol. Lett. **11**, 674 (1999).

[3] *Supercontinuum Generation in Optical Fibers*, edited by J. M. Dudley and J. R. Taylor (Cambridge University Press, Cambridge, England, 2010).

[4] S. Xu, D. H. Reitze, and R. S. Windeler, Opt. Express **12**, 4731 (2004).

[5] B. von Vacano, W. Wohlleben, and M. Motzkus, Opt. Lett. **31**, 413 (2006).

[6] D. Lorenc, D. Velic, A. N. Markevitch, and R. J. Levis, Opt. Commun. **276**, 288 (2007).

[7] G. A. Siviloglou, J. Broky, A. Dogariu, and D. N. Christodoulides, Phys. Rev. Lett. **99**, 213901 (2007).

[8] A. Chong, W. H. Renninger, D. N. Christodoulides, and F. W. Wise, Nat. Photon. **4,** 103 (2010).

[9] D. Abdollahpour, S. Suntsov, D. G. Papazoglou, and S. Tzortzakis, Phys. Rev. Lett. **105,** 253901 (2010).

[10] A. V. Husakou and J. Herrmann, Phys. Rev. Lett. **87,** 203901 (2001).

[11] M. Miyagi and S. Nishida, Appl. Opt. **18,** 2237 (1979).

[12] J. C. Travers, M. H. Frosz, and J. M. Dudley, ''Nonlinear fibre optics overview'', in [3], p. 46.

[13] G. Genty, M. Lehtonen, and H. Ludvigsen, Opt. Express **12,** 4614 (2004).

[14] D. R. Austin, C. M. de Sterke, B. J. Eggleton, and T. G. Brown, Opt. Express **14,** 11997 (2006).

[15] J. Durnin, J. J. Miceli, Jr., and J. H. Eberly, Phys. Rev. Lett. **58,** 1499 (1987).